Journal of Inflammation Research

Dovepress
open access to scientific and medical research

Open Access Full Text Article

ORIGINAL RESEARCH

LPS-Induced Activation of the cGAS-STING Pathway is Regulated by Mitochondrial Dysfunction and Mitochondrial DNA Leakage in Endometritis

Mu-zi Li[1–5], Xiao-yang Wen[1–5], Xiao-qiang Liu[1–6], Yu-qing Wang[1–5], Lei Yan[1–5]

[1]Center for Reproductive Medicine, Shandong University, Jinan, People's Republic of China; [2]Key Laboratory of Reproductive Endocrinology of Ministry of Education, Shandong University, Jinan, People's Republic of China; [3]Shandong Key Laboratory of Reproductive Medicine, Jinan, People's Republic of China; [4]Medical Integration and Practice Center, Shandong University, Jinan, People's Republic of China; [5]Reproductive Hospital Affiliated to Shandong University, Jinan, People's Republic of China; [6]Reproductive Medicine Center, Qingdao Women and Children's Hospital, Qingdao, People's Republic of China

Correspondence: Lei Yan, Email yanlei@sdu.edu.cn

Introduction: Chronic endometritis is a common disease in women of childbearing age and can cause pelvic inflammatory disease. The cGAS-STING pathway plays an important role in many inflammatory diseases.

Purpose: The aim of this study was to investigate the relationship between the cGAS-STING pathway and endometritis.

Methods: We collected endometrium samples from patients with endometritis to detect changes in the cGAS-STING pathway. In vitro, human endometrial stromal cells (HESC) were stimulated with lipopolysaccharide (LPS), and a mouse *STING* gene-knockout model was established by CRISPR/cas9 for STING to further explore the mechanism underlying its effects in endometritis. We used Western blotting (WB) and immunohistochemical staining to detect the variations in protein levels and real-time PCR to study the variations in gene expression.

Results: We observed the activation of the cGAS-STING pathway and an increase in the expression of cytokine-encoding genes, including *IL-8, IL-6, IL-1β*, and *IFN-β1*, in endometrial tissues of patients with endometritis. Stimulation of HESCs using LPS demonstrated increase in the expression of proteins involved the cGAS-STING pathway and the gene expression of inflammatory cytokines. STING-knockdown experiments demonstrated a decrease in the gene expression levels of inflammatory cytokines. Moreover, we also identified the translocation of IRF3 and STING after LPS stimulation. Regarding mitochondrial function, LPS led to an increase in reactive oxygen species levels and a reduction in mitochondrial membrane potential. However, we observed that the mitochondrial DNA (mtDNA) leaked into the cytoplasm, upregulating the levels of proteins involved in the cGAS-STING pathway upon LPS stimulation. Furthermore, our results showed that LPS induced hyperemia, inflammatory factor production, and expression of Pho-TBK1 in wild-type mice compared with the levels in control mice, and *STING* gene-knockdown alleviated these effects.

Conclusion: LPS induces mitochondrial dysfunction in endometrial stromal cells, resulting in mtDNA leakage and promoting endometritis by stimulating the cGAS-STING pathway.

Keywords: endometritis, cGAS-STING, lipopolysaccharide, mitochondrial dysfunction, mitochondrial DNA, inflammatory factors

Introduction

Chronic endometritis (CE) is an infectious and inflammatory lesion of the endometrium caused by pathogenic bacteria. Apart from its subtle symptomatology, patients with CE could suffer from infertility and benefit less from assisted reproductive technology.[1–3] Additionally, a population with CE was identified to have consequential repeated implantation failure.[2,4,5]

The cyclic GMP–AMP synthase (cGAS)-STING pathway has been thought to vitally participate in inflammatory diseases, and this pathway has been regarded as an important therapeutic target based on various studies.[6,7] cGAS undergoes a conformational change to an active state and forms the second messenger cyclic GMP–AMP (cGAMP) from ATP and GTP after associating with DNA and the cyclic-dinucleotide sensor STING will subsequently detect these

Received: 24 May 2022
Accepted: 28 September 2022
Published: 5 October 2022

changes and becomes activated.[8] STING is mainly located in the endoplasmic reticulum (ER) and can phosphorylate TANK-binding kinase 1 (TBK1) and interferon (IFN) regulatory factor (IRF3) to regulate inflammation.[6] However, the precise cGAS-STING pathway regulatory mechanisms in CE remain unclear.

Studies have verified that many diseases, such as amyotrophic lateral sclerosis, odontoblast inflammation, and hypertensive inflammation, are related to mitochondrial dysfunction and mitochondrial DNA (mtDNA) leakage.[9–11] Many studies have also illustrated that cGAS can be activated by endogenous DNA.[12,13] Despite our increasing understanding of the links among the cGAS-STING pathway, mitochondrial dysfunction, and inflammatory diseases, the nature of such associations in endometritis remains a major unanswered question.

Further, lipopolysaccharide (LPS), the endotoxin produced by gram-negative bacteria, can enter the body to induce the production of inflammatory factors. LPS have been used to mimic the effects of gram-negative pathogens and establish models of inflammation, including endometritis.[14–16] Considering the importance of the cGAS-STING pathway and mitochondrial dysfunction in inflammatory diseases, the objective of this study was to determine whether both take part in the regulatory mechanisms of LPS-induced endometritis. We also sought to verify whether the cGAS-STING pathway can be activated by endogenous mtDNA in human endometrial stromal cells (HESCs).

Materials and Methods

Cell Culture and Cell Stimulation

HESCs were cultured at 37 °C with 5% of CO_2 in DMEM/F12 (21,041,025, Gibco, USA) medium containing 10% fetal bovine serum (04–001-1A, Biological Industries, USA). When the cell density was greater than 90%, cells were passaged at a ratio of one to three. We used cells from passages 2–15. The culture medium was routinely changed every 2 days. LPS (S1372, Beyotime, China) was added to the culture medium at a suitable concentration. STING–homo-679 (GenePharma, China) and Lipofectamine 3000 (L3000015, Thermo Fisher Scientific, USA) were used to transfect HESCs.

Animals

Female and male C57BL/6JGpt mice (5 weeks of age) were purchased from Gempharmatech Co., Ltd. All mice were housed in a specific-pathogen-free environment (humidity, 50 ± 5%; temperature, 20–22 °C). Endometritis mouse models (10–12 weeks of age; weight, 18–22 g) were induced via LPS intrauterine infusion (1 mg/kg) as described in a previous study.[17,18] The CRISPR/cas9 knockout target site in *Sting1* was designed using the CRISPR Design website of the Massachusetts Institute of Technology (http://crispor.tefor.net/). The target genes were verified by PCR to confirm the accuracy of gene sequences near the target sites. Primers included the following: PCR① T036783-F1, ACCTGATGGGAGGTATCTACCGG; T036783-R1, CCAGCAACTAGCATCAGAACCTCC; PCR② T036783-F2, GGTGCCTGACAACCTGAGTGTAG; T036783-R2, CCTCAATGCTCTCATAGCCTTCAC.

Sampling of Endometrium and Diagnosis

All patients underwent hysteroscopy at the follicular stage of the menstrual cycle (3−7 days after menstruation). Iodophor cotton was placed in the vaginal speculum to clean the cervix, and the uterine cavity was expanded with 0.9% saline. The cervical canal, uterine cavity, cornua, and finally the fundus and left and right front and rear walls were explored. The endometrium of the corresponding site of endometrial congestion was scraped with a sharp curette to improve the accuracy of the biopsy and avoid unnecessary curettage.[19] After hysteroscopy and the endometrial biopsy, CD138 immunohistochemistry was performed on all extracted patient endometrial tissues to determine the CE diagnosis. CE was diagnosed when ≥5 typical plasma cells were observed in the endometrial stroma based on a 10×400 magnification, and the absence of CE was determined when no typical plasma cells were found in the endometrium.

RNA Extraction and Real-Time PCR

TRIzol Reagent (15,596,018, Ambion, USA) was used with the HESCs, human endometrial tissue, and mouse uterus tissues. Cells were washed with cold phosphate-buffered saline (PBS) twice, and 1 mL of TRIzol was added to each well

of a six-well culture plate. Cells were ground thoroughly, and the liquid was transferred to a 1.5 mL RNase/DNase-free microcentrifuge tube and let stand for 10 min at room temperature. Then, 200 μL of chloroform was mixed with the liquid and incubated at room temperature for 3 min. The liquid was centrifuged at 12,000 rpm for 15 min at 4 °C, and the supernatant was transferred to an RNase/DNase-free microcentrifuge tube. Next, 500 μL of isopropanol was mixed with the supernatant and set it aside for 10 min at room temperature. The mixture was centrifuged for 10 min at the same rotating speed and temperature as noted previously in this section. The supernatant was removed, and the pellet was washed with 75% ethanol. The pellet was centrifuged at 7500 rpm for 5 min at 4 °C, the supernatant was removed, and the sample was dried for 10 min. Finally, 1% DEPC (R1600, Solarbio, China) was added to dissolve the RNA pellet. The extracted RNA was subjected to the real-time PCR using the TaKaRa PrimeScriptTM RT reagent Kit with gDNA Eraser (RR047Q, Takara, China). All primers are listed in the Supplementary Table 1(BioSune, China).

Western Blotting Analysis

RIPA Lysis Buffer (P0013B, Beyotime, China) or the Minute™ Total Protein Extraction Kit for Animal Cultured Cells/Tissues (SD-001/SN-002, Invent Biotechnologies, Beijing, China) was used to collect examples in RNase/DNase-free microcentrifuge tubes, and the Protease/Phosphatase Inhibitor Cocktail (100×; #5872, Cell Signaling Technology, USA) was regularly added. Examples were centrifuged at 15,000 rpm at 4 °C for 15 min. The supernatant was transferred to new RNase/DNase-free microcentrifuge tubes, to which Loading Buffer (5×; P0015L, Beyotime, China) was added; the samples were then placed in a 100 °C water bath for 15 min. The proteins were separated with a 4–20% Precast Protein Gel 15 Wells (SLE009, Smart Lifesciences, China) and transferred to an Immobilon-P Transfer Membrane (IPVH00010, Merck, USA). The membranes were blocked with QuickBlock™ Blocking Buffer for Western Blot (P0252, Beyotime, China) for 20 min and washed three times with Tris-buffered saline with Tween solution for 10 min and then immunoblotted overnight at 4 °C with specific primary antibodies. The antibodies used for this assay were as follows: anti-GAPDH (1:10000, 60004-1-Ig, Proteintech, USA); anti-tubulin (1:10000, 66031-1-Ig, Proteintech, USA); anti-Lamin B1 (1:10000, 66095-1-Ig, Proteintech, USA); anti-cGAS (1:1000, 83623, Cell Signaling Technology, USA); anti-STING (1:1000, 66680-1-Ig, Proteintech, USA; 1:1000, 13647, Cell Signaling Technology, USA), anti-TBK1 (1:1000, 38066, Cell Signaling Technology, USA); anti-Pho-TBK1 (1:1000, 5483, Cell Signaling Technology, USA); anti-IRF3 (1:1000, ab68481, Abcam, UK); anti-Pho-IRF3 antibody (1:1000, 11904, Cell Signaling Technology, USA); anti-Pho-IRF-3 (1:1000, 29047, Cell Signaling Technology, USA); horseradish enzyme-conjugated goat anti-rabbit IgG (H+L) (1:5000, ZB-2301, ZSGB-BIO, China); horseradish enzyme-conjugated goat anti-mouse IgG (H+L) (1:5000, ZB-2305, ZSGB-BIO, China). After the membranes were washed three times, they were incubated with the secondary antibody for 1 h at room temperature. Clarity Western ECL Substrate (1705061, BIO-RAD, USA) was used to visualize and quantify the immunoblot.

Immunofluorescence Staining

The culture medium was removed from the culture dishes after cell growing on the glass slide, and the cells were washed twice with PBS. Then, 4% Paraformaldehyde Fix Solution (P0099, Beyotime, China) was added for 20 min at room temperature, and cells were washed with PBS. Next, 10% goat serum (ZLI-9022, Origene, USA) +0.3% Triton-X-100 (T8200, Solarbio, China) +PBS was used for permeabilization and blocking for 1 h. After removing the liquid, samples were incubated with specific primary antibodies (as noted previously herein) at 4 °C overnight in a wet box. The primary antibodies were diluted to 1:200 with 10% goat serum+0.3% Triton-X-100+PBS. Samples were washed three times with PBS, and the secondary antibodies were applied in a wet box for 1 h at room temperature in the dark. Secondary antibodies (4412 and 8889, Cell Signaling Technology, USA) were diluted at 1:800 in PBS+0.1% Triton-X-100. Samples were washed three times with PBS. ProLong™ Gold Antifade Mountant with DAPI (P36935, Invitrogen, USA) was added to the slides, which were observed and photographed under a confocal microscope.

Immunohistochemical Staining

Paraffin sections were dewaxed using xylene, followed by hydration with absolute ethanol, 95% ethanol, and 75% ethanol. Antigen retrieval was performed by boiling the specimen at 100 °C for 15 min using Sodium Citrate Antigen

Retrieval Solution (50×; C1032, Solarbio, China). After cooling, permeabilization, blocking, and primary antibody application were the same as previously described herein. The Rabbit Two-step Detection Kit (PV-9001, ZSGB-BIO, China) and DAB Chromogenic Kit (ZLI-9018, ZSGB-BIO, China) were used according to the instruction manuals. The samples were then stained with hematoxylin, dehydrated with 95% ethanol and absolute ethanol, cleared with xylene, and finally mounted with neutral balsam (96949–21-2, Solarbio, China). They were observed and photographed under an optical microscope.

Mitochondrial Function Assay

Cells were seeded in confocal culture dishes (FCFC016, Beyotime, China) and cultured overnight. For reactive oxygen species (ROS) assays, 5 mM DCFH-DA (D6470, Solarbio, China) was added to the DMEM/F12 medium at a ratio of 1:1000 (v/v), and the mixture was incubated at 37 °C for 15 min in the dark. The DCFH-DA was washed with preheated PBS twice, and samples were observed and photographed under an optical microscope. For the mitochondrial membrane potential (MMP) assay, cells were stained with JC-10 following the manufacturer's instruction (CA1310, Solarbio, China). Then, the samples were tested using a Confocal Laser Scanning Microscope.

Mitochondrial DNA Isolation and Transfection

mtDNA was isolated from cells using the Mitochondria DNA Isolation Kit (K280, BioVision, USA) following the instructions of the manufacturer. The concentration of mtDNA was measured using a NanoDrop™ One/OneC (ND-ONE -W, Thermo Fisher Scientific, USA). Lipofectamine 3000 was dissolved in the DMEM/F12 medium containing 10% fetal bovine serum and allowed to stand at room temperature for 5 min, while mtDNA or TE Buffer were respectively dissolved in the DMEM/F12 medium containing 10% fetal bovine serum. After standing, Lipofectamine 3000 was mixed with mtDNA or TE Buffer respectively and continued standing at room temperature for 15 min. If the density of HESCs in the six-well plate exceeds 90%, replace 1.5mL of DMEM/F12 medium containing 10% fetal bovine serum in each well in advance, and add the mtDNA or TE Buffer mixed with lipofectamine 3000 0.5 mL to the six-well plate.

Statistics

Statistical analyses were performed using an unpaired two-tailed Student's *t*-test with GraphPad prism 9. *P*-values less than 0.05 indicated a significant difference.

Results

Enhanced cGAS-STING Pathway and Inflammatory Factor Levels in Patients with Endometritis

First, the levels of cGAS-STING pathway proteins, including cGAS, STING, Pho-TBK1, IRF3, and Pho-IRF3 were apparently increased, whereas those of TBK1 did not show a significant difference, in the endometrium of patients with endometritis compared with those in the normal group (Figure 1A and B). Figure 1C shows that endometritis also contributed to the higher STING protein levels in the endometrium. Next, real-time PCR was conducted to detect genes encoding the related inflammatory factors. *IL-8, IL-1β, IFN-β1*, and *IL-6* expression levels were significantly higher in endometritis tissues (Figure 1D). Together, these data indicated that the cGAS-STING pathway is involved in the mechanisms regulating endometritis.

LPS Induces the Production of Inflammatory Factors Involved in cGAS-STING Pathway Activation in HESCs

LPS is regarded as a common molecule used to generate endometritis models. In our study, we found that LPS can lead to enhanced production of inflammatory factors, including IL-8, IL-1β, IFN-β1, and IL-6, in HESCs after 6 h (Figure 2A). In addition, activation of the cGAS-STING pathway was also found after adding LPS for 2 h, as cGAS, Pho-TBK1, and Pho-IRF3 levels were increased significantly (Figure 2B and C). We next transfected HESCs with small interfering RNA STING or the negative control and detected the aforementioned inflammatory factors after LPS

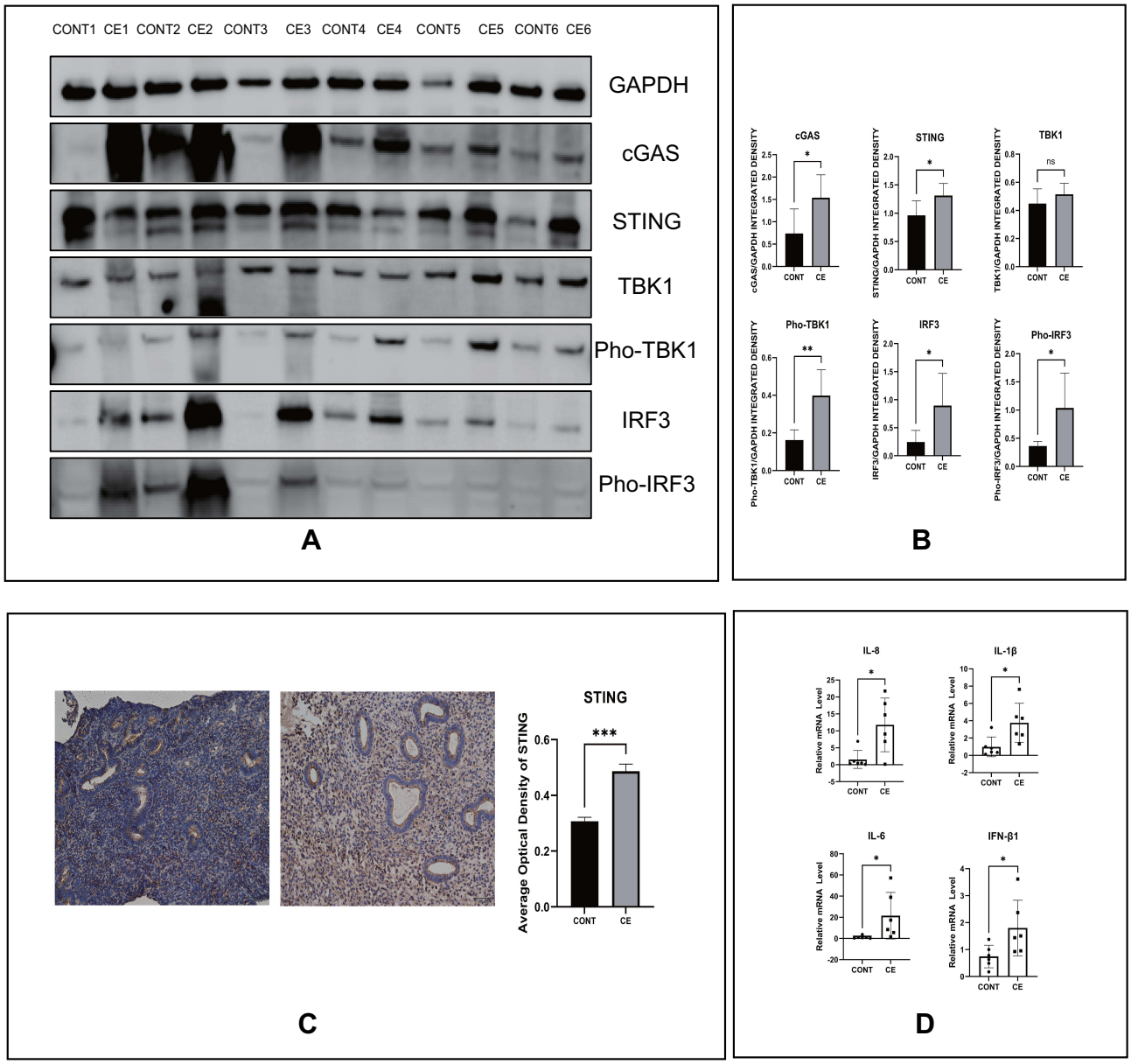

Figure 1 Enhanced cGAS-STING pathway and inflammatory factor levels in patients with endometritis. (**A**) The protein levels of the cGAS-STING pathway by Western blot in indicated groups. (**B**) Quantitative analysis of (**A**). (**C**) The protein levels of STING by IHC in indicated groups and their quantitative analysis. (**D**) The relative mRNA levels of IL-8, IL-1β, IL-6 and IFN-β1 by RT-PCR in indicated groups. (*p < 0.05, **p < 0.01, ***p < 0.001).

stimulation. Expression of these inflammatory factors tended to be reduced in the STING-knockdown group, as see in Figure 2D. This result further proved that the cGAS-STING pathway participates in the LPS-induced inflammatory mechanisms in HESCs in vitro.

LPS Induces STING Undergoing Perinuclear Transfer and IRF3 Transferring from the Cytoplasm to the Nucleus

As indicated, we found that LPS could activate the cGAS-STING pathway. Next, we further explored whether the location of related proteins in this pathway would change under these conditions. Immunofluorescence staining was conducted, and we found that the green fluorescence signal representing STING encompassed the nucleus and that the red fluorescence signal representing IRF3 was increased in the nucleus (Figure 3A and B). In addition, cytoplasmic and nuclear proteins were isolated from each other, and Western blotting was performed to verify the change in the location of these molecules. As seen

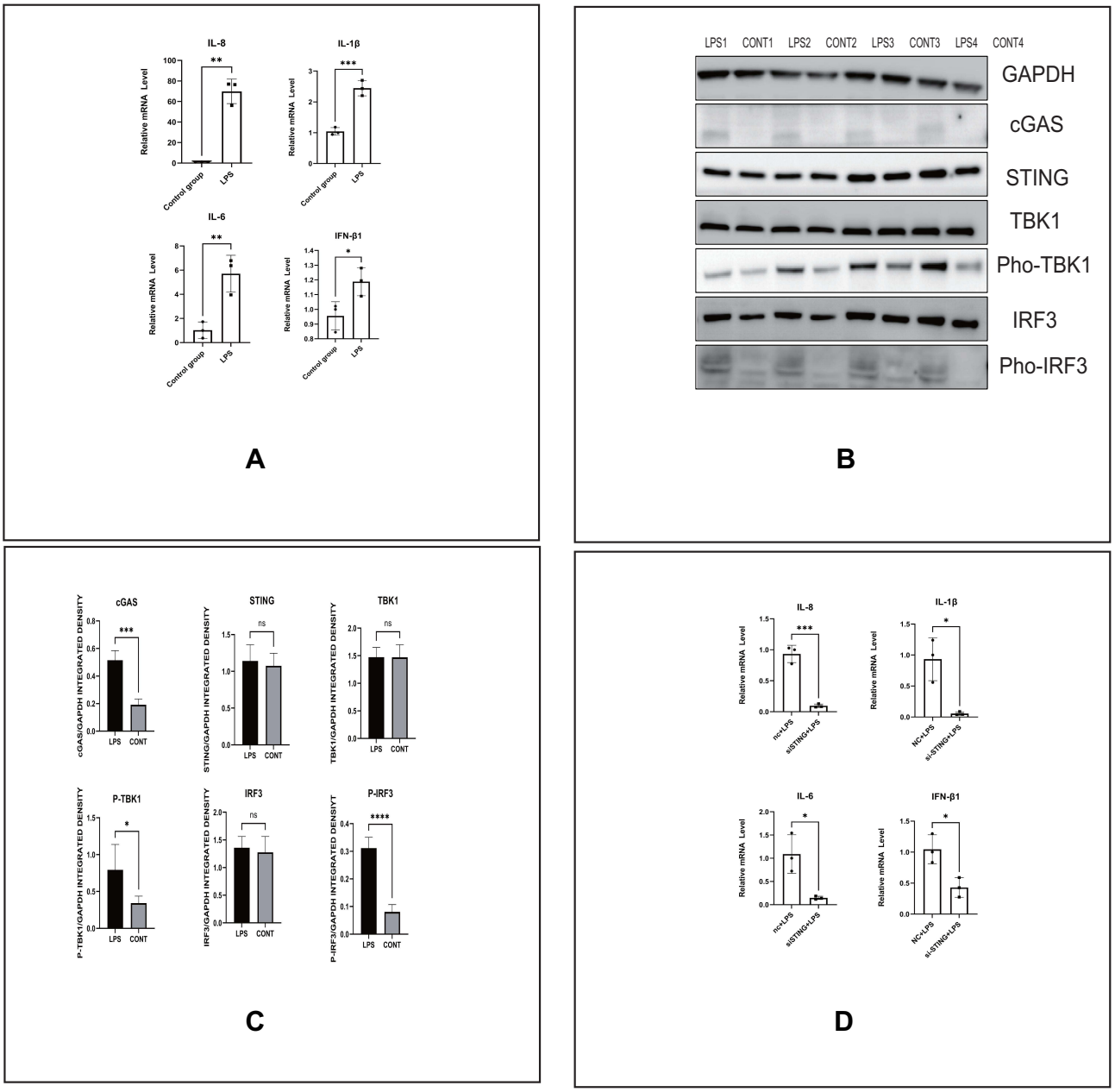

Figure 2 LPS induces the production of inflammatory factors involved in cGAS-STING pathway activation in HESCs. (**A**) The relative mRNA levels of IL-8, IL-1β, IL-6 and IFN-β1 by RT-PCR in indicated groups of HESCs. (**B**) The protein levels of the cGAS-STING pathway by Western blot in indicated groups of HESCs. (**C**) Quantitative analysis of (**B**). (**D**) The relative mRNA levels of IL-8, IL-1β, IL-6 and IFN-β1 by RT-PCR in indicated groups of HESCs. (*p < 0.05, **p < 0.01, ***p < 0.001, ***p < 0.0001).

in Figure 3C and E, IRF3 levels were clearly enhanced in the nucleus but STING levels did not significantly change after LPS stimulation. These results demonstrated that the perinuclear translocation of STING and intranuclear translocation of IRF3 participate in activation of the cGAS-STING pathway in HESCs after LPS stimulation.

LPS Activates the cGAS-STING Pathway by Inducing Mitochondrial Dysfunction

Previous studies have found that mitochondrial functions are linked to LPS.[12,13] mtDNA leaking into the cytoplasm was found to result in activation of the cGAS-STING pathway. To determine whether this would occur in HESCs, we used LPS to stimulate these cells and detected mitochondrial functions. The ROS green fluorescence signal was markedly increased, as shown in Figure 4A, after adding LPS. Under the same treatment conditions, we measured the difference in the MMP, and Figure 4B shows that the ratio of green fluorescence intensity to red fluorescence intensity was

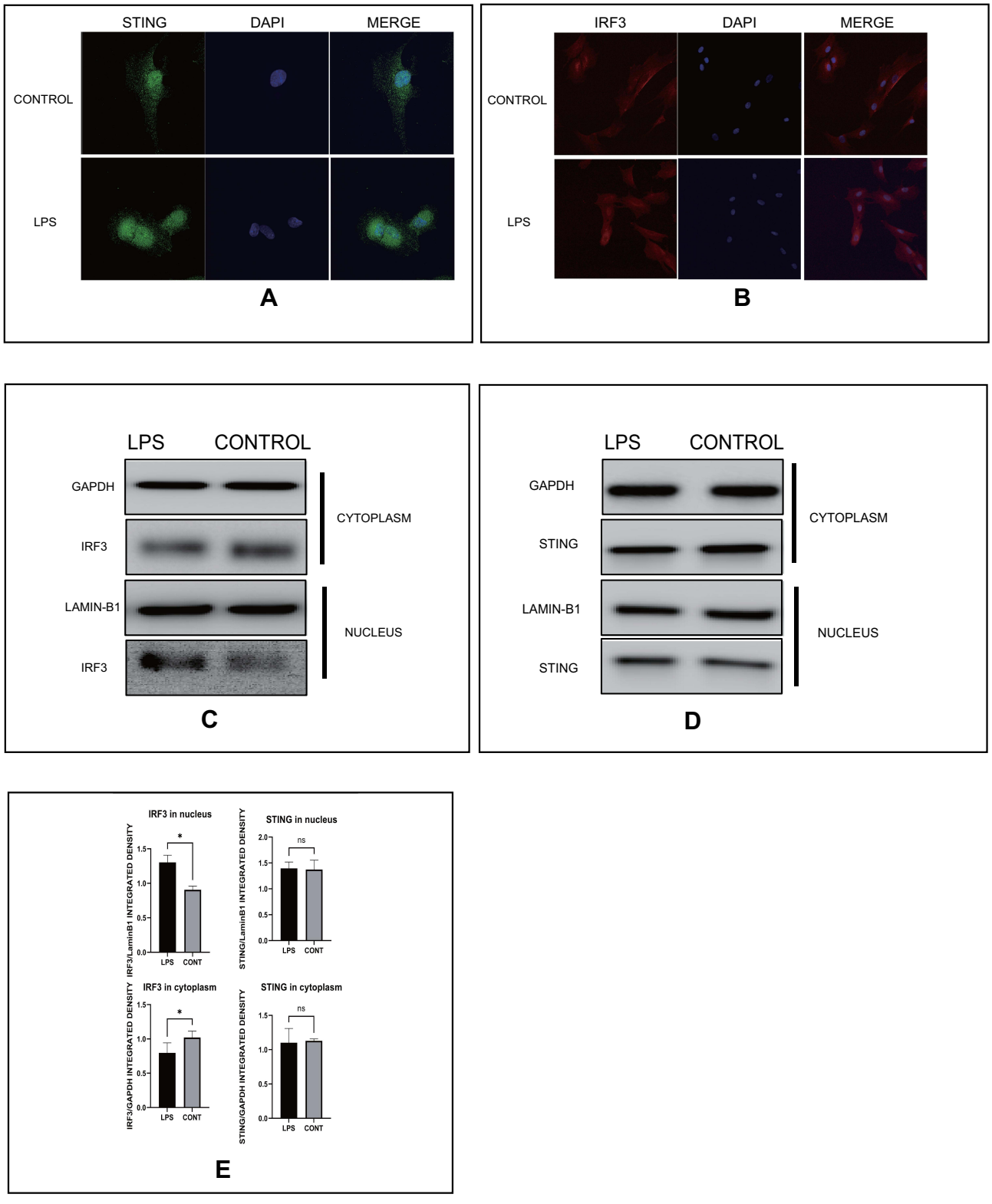

Figure 3 LPS induces STING undergoing perinuclear transfer and IRF3 transferring from the cytoplasm to the nucleus. (**A**) Representative images of immunofluorescence of STING in indicated groups of HESCs. (**B**) Representative images of immunofluorescence of IRF3 in indicated groups of HESCs. (**C**) The protein levels of IRF3 in cytoplasm and nucleus of HESCs in indicated groups by Western blot. (**D**) The protein levels of IRF3 in cytoplasm and nucleus of HESCs in indicated groups by Western blot. (**E**) Quantitative analysis of (**C** and **D**). (*$p < 0.05$).

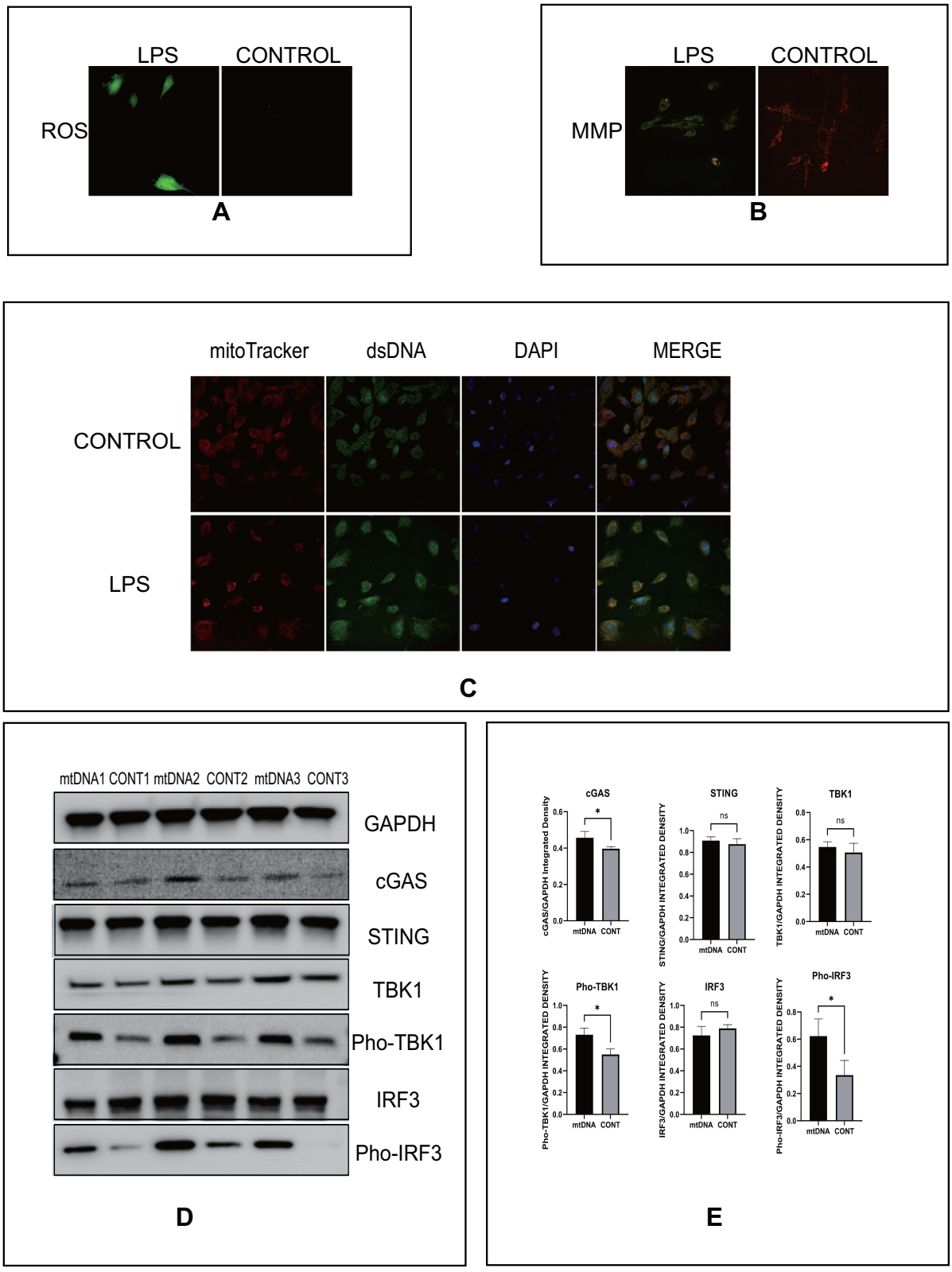

Figure 4 LPS activates the cGAS-STING pathway by inducing mitochondrial dysfunction. (**A**) Representative images of immunofluorescence of ROS (red) indicated groups of HESCs. (**B**) Representative images of immunofluorescence of MMP (red and green) indicated groups of HESCs. (**C**) Representative images of DAPI (blue), mitochondria (red), and dsDNA (green) in indicated groups of HESCs, p<0.05. (**D**) The protein level of the cGAS-STING pathway by Western blot in indicated groups of HESCs. (**E**) Quantitative analysis of (**D**). (*p < 0.05).

significantly increased compared with that in the control group. We also detected mtDNA levels in the cytoplasm after LPS stimulation, and the results in Figure 4C demonstrated the dsDNA levels were higher after stimulation. We next extracted mtDNA from HESCs and transfected it into cells. As speculated, mtDNA, at 1 μg/mL, could lead to significant increases in the protein levels of cGAS, Pho-TBK1, and Pho-IRF3 (Figure 4D). These results showed that LPS can induce mitochondrial dysfunction, releasing mtDNA to activate the cGAS-STING pathway.

Intrauterine Infusion of LPS Induces Uterine Hyperemia and cGAS-STING Pathway Activation in Mice

To verify that LPS can activate the cGAS-STING pathway in vivo, we perfused the uterine cavity of mice with LPS at a rate of 1 mg/kg. We dissected mice treated at a different time points and found that LPS could induce uterine hyperemia to a certain extent in both wild-type (WT) and STING-knockout mice, but the degree of hyperemia in knockout mice was milder and recovery was faster. As seen in Figure 5A, in WT mice treated with LPS for 6 and 12 h, uterine hyperemia was obvious, and after 24 h of LPS treatment, this condition was alleviated. However, the uterine hyperemia in the STING-knockout mice was more obvious only after 6 h of LPS treatment, and this condition was milder after treatment for 12 and 24 h. Figure 5B shows that LPS up to 12 h could increase the RNA levels of inflammatory factors and that knocking out STING could prevent this phenomenon (Figure 5C). As shown in Figure 5D and E, the protein expression of pho-TBK1 was significantly increased up to 6 h after adding LPS to WT mice; however, it was obviously reduced to basal levels when *STING* was knocked out. These results in vivo further proved that STING is involved in the LPS-induced inflammatory effects in the endometrium.

Discussion

Here, to our best knowledge, this was the first study to discover activation of the cGAS-STING pathway in endometritis. Moreover, our research comprehensively elucidated this mechanism using three approaches, specifically human tissues, animals, and cells. As shown in Figure 6, this study unveiled an unprecedented cellular response to LPS stimulation associated with endometritis. Mitochondrial function can be disturbed by LPS, causing ROS increases and MMP decreases; meanwhile, the release of mtDNA into the cytoplasm activates the cGAS-STING pathway, which is accompanied by the perinuclear translocation of STING and the nuclear transfer of IRF3. This ultimately activates the inflammatory cytokines IL-8, IL-1β, IL-6, and IFN-β1 in LPS-induced HESCs. Moreover, STING abrogation decreased the release of inflammatory factors both in HESCs and STING-knockout mice. Therefore, therapeutic strategies focusing on mitochondrial conservation and the cGAS-STING pathway might be feasible to mitigate the effects of bacterial attack on the endometrium.

The C-terminal part of cGAS, containing the nucleotidyltransferase domain, bears positively charged DNA-binding sites, including one primary site and two additional sites, which bind the sugar-phosphate backbone of DNA.[6] As a DNA sensor, dsDNA can result in the enzymatic activation of cGAS and the synthesis of cGAMP. This cGAMP, as a second messenger, binds to the ER-localized adaptor protein STING, causing it to translocate from the ER to the Golgi.[20] In our present study, we found that mtDNA stimulation, mediated by LPS, can enhance the amount of cGAS in HESCs by Western blotting. At the same time, STING was also translocated into the perinuclear region in HESCs after LPS stimulation based on immunofluorescence. This phenomenon was also discovered in microvascular endothelial cells, neonatal rat cardiomyocytes, and H9c2 cells, but unfortunately we did not show the precise position of STING in the ER and Golgi.[21,22] STING, activated by viruses or endogenous DNA, recruits and phosphorylates TBK1 and the transcription factor IRF3 to induce type-I interferons and other cytokines.[12,13,23] The activated cGAS-STING pathway and the upregulated phosphorylation levels of TBK1 and IRF3 will further participate in inflammation, apoptosis, and pyroptosis to regulate inflammatory diseases and cancer.[24–28] An increase in the amount of pho-TBK1 and pho-IRF3 was observed after LPS or mtDNA stimulation in HESCs in our study, and at the same time, the nuclear translocation of IRF3 was observed by immunofluorescence. Further, levels of IFN-β1 and other related inflammatory cytokines, including IL-8, IL-1β, and IL-6, were shown to be increased with LPS stimulation both in vivo and vitro, and STING deficiency reduced the

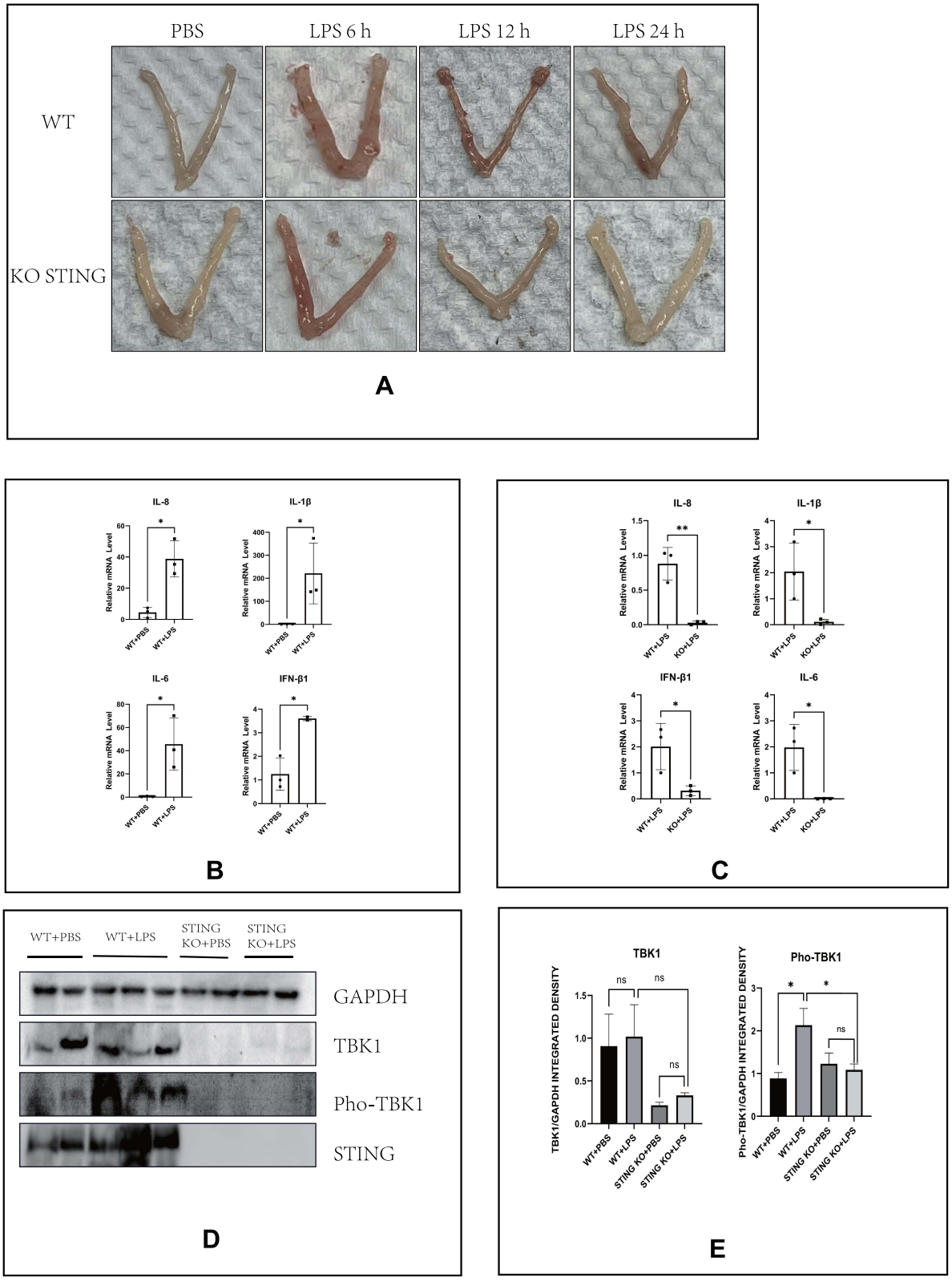

Figure 5 Intrauterine infusion of LPS induces uterine hyperemia and cGAS-STING pathway activation in mice. (**A**) Representative images of the uterus of mice after intrauterine infusion in indicated groups. (**B**) The relative mRNA levels of IL-8, IL-1β, IL-6, and IFN-β1 by RT-PCR in indicated groups of the uterus of mice (LPS: 12 h). (**C**) Quantitative analysis of (**B**). (**D**) The protein levels of TBK1 and Pho-TBK1 (LPS: 6 h). (**E**) Quantitative analysis of (**D**). (*p < 0.05).

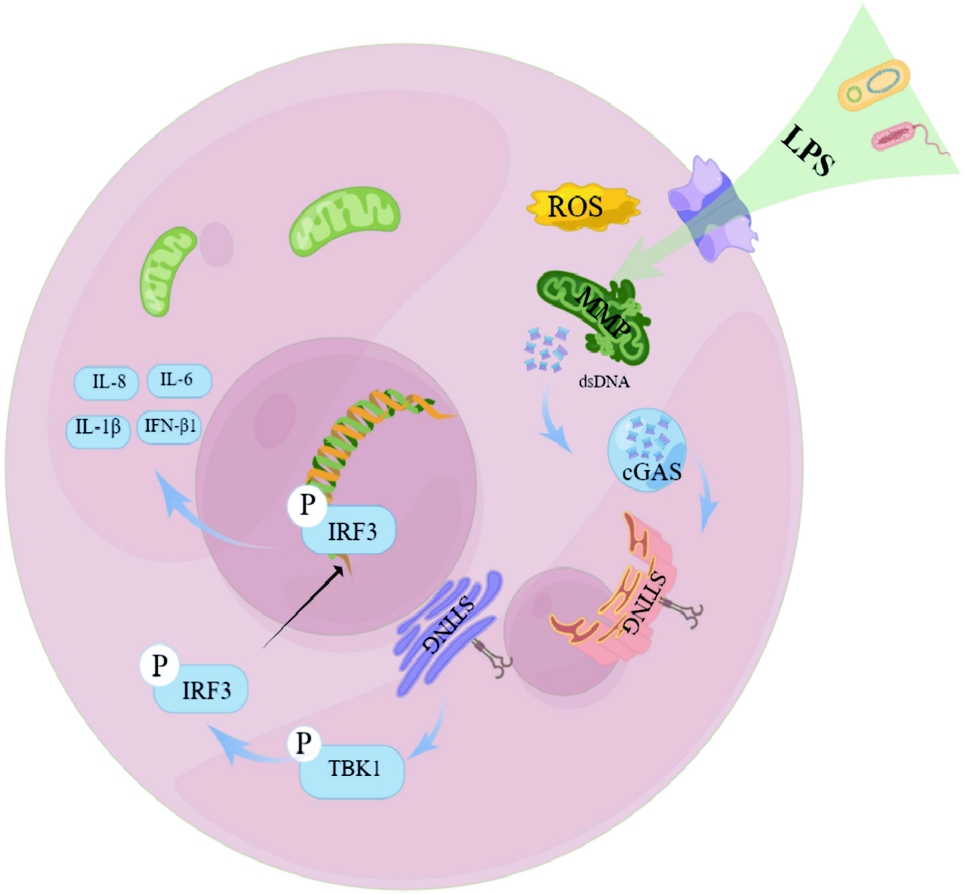

Figure 6 A putative scheme explaining the mechanism by which mitochondrial dysfunction, mtDNA leakage, and cGAS-STING pathway regulate endometritis induced by LPS.

levels of IFN-β1 and other inflammatory cytokines. These results suggested that the cGAS-STING-TBK1-IRF3 axis participates in the pathology of CE.

Mitochondria not only maintain classic cellular production but also play an important role in other processes, such as cellular metabolism and interactions with the lysosome.[29,30] Disruptive ROS and changes to the MMP are considered common forms of mitochondrial dysfunction.[31,32] In addition, mtDNA leakage into the cytoplasm also occurs in some diseases involving mitochondrial damage, like acute kidney injury.[33] In our study, we showed that ROS levels increased and MMP decreased in response to LPS, and simultaneously mtDNA leakage into the cytoplasm occurred based on immunofluorescence, which indicated that mitochondrial dysfunction is involved in the mechanisms underlying endometritis.

There were some limitations in this study. First, many researchers have demonstrated that mitochondrial permeability transition pores or some other proteins participate in mitochondrial dysfunction.[34,35] Our study did not address these aspects and only assessed mitochondrial function. Further, we did not precisely limit the estrous cycle in mice and when generating the HESCs from mice in our experiments. As such, the expression levels of cGAS-STING pathway components could be affected by the mouse physiological cycle. In addition, we only detected the expression of inflammation factors in cells and tissues, but not addressed the release of inflammatory factors. Despite these limitations, we suggest that some aspects of our work are still worthy of further study. Our study showed that the protein level of STING was increased in endometrial tissue between the endometritis and the control groups, but we did not find any difference in HESCs after LPS stimulation. Many types of inflammatory cells exist in the endometrium. Whether the difference in STING expression between endometrial tissue and HESCs is caused by inflammatory cells is worthy of further exploration. In addition, it is still not clear how IRF3 enters the nucleus to regulate the expression of inflammatory

factors in endometritis. At last, Considering the absence of a clear understanding of chronic endometritis diagnosis, we still need to further explore the diagnostic criteria of endometritis to facilitate the management and treatment of patients.[36,37]

Conclusion

Although there have been several studies on the cGAS-STING pathway in cancer or other inflammatory diseases, to our knowledge, this study was the first to show that the cGAS-STING pathway can regulate inflammatory mechanisms in non-inflammatory cells, specifically HESCs, in endometritis.[24–28] In addition, we also found that LPS can induce an increase in ROS levels and a decrease in MMP and lead to mtDNA leakage into the cytoplasm, which indicates the occurrence of mitochondrial dysfunction in endometritis. Moreover, we showed that the mtDNA of HESCs can activate the cGAS-STING pathway. Our findings suggest that mitochondrial dysfunction, mtDNA leakage, and the cGAS-STING pathway are three important factors in endometritis that could be targeted for treatment.

Data Sharing Statement

The primary data for this study is available from the authors on direct request.

Ethics Approval and Consent to Participate

All animal procedures were approved by the Reproductive Hospital Affiliated to Shandong University institutional review board ([2022] IRB No.(16)). The experiments were performed complying with the Declaration of Helsinki, following the experimental and welfare guidelines of Shandong University. Written informed consent was obtained from all participants at the time of presentation for hysteroscopy treatment.

Acknowledgments

The authors thank our patients and all participants in the data collection. Special thanks to professor Yan Jie from Shandong University for providing guidance on our experimental design. Thank our colleagues at Medical Integration and Practice Center, Shandong University, Jinan Shandong, China for assistance with sample collection. We are grateful to Dr. Lei Yan, Jie Yan and other colleagues for help with the experimental protocol.

Author Contributions

All authors made a significant contribution to the work reported, whether that is in the conception, study design, execution, acquisition of data, analysis and interpretation, or in all these areas; took part in drafting, revising or critically reviewing the article; gave final approval of the version to be published; have agreed on the journal to which the article has been submitted; and agree to be accountable for all aspects of the work.

Funding

This study was founded by National Natural Science Foundation of China. (Grant no. 82071617).

Disclosure

The authors report no conflicts of interest in this work.

References

1. Cicinelli E, Matteo M, Tinelli R, et al. Prevalence of chronic endometritis in repeated unexplained implantation failure and the IVF success rate after antibiotic therapy. *Hum Reprod*. 2015;30(2):323–330. doi:10.1093/humrep/deu292
2. Cicinelli E, Matteo M, Trojano G, et al. Chronic endometritis in patients with unexplained infertility: prevalence and effects of antibiotic treatment on spontaneous conception. *Am J Reprod Immunol*. 2018;79(1):e12782. doi:10.1111/aji.12782
3. Vitagliano A, Saccardi C, Noventa M, et al. Effects of chronic endometritis therapy on in vitro fertilization outcome in women with repeated implantation failure: a systematic review and meta-analysis. *Fertil Steril*. 2018;110(1):103–112 e1. doi:10.1016/j.fertnstert.2018.03.017
4. Kitaya K, Matsubayashi H, Takaya Y, et al. Live birth rate following oral antibiotic treatment for chronic endometritis in infertile women with repeated implantation failure. *Am J Reprod Immunol*. 2017;78(5):e12719. doi:10.1111/aji.12719

5. Bouet PE, El Hachem H, Monceau E, Gariepy G, Kadoch IJ, Sylvestre C. Chronic endometritis in women with recurrent pregnancy loss and recurrent implantation failure: prevalence and role of office hysteroscopy and immunohistochemistry in diagnosis. *Fertil Steril*. 2016;105 (1):106–110. doi:10.1016/j.fertnstert.2015.09.025
6. Decout A, Katz JD, Venkatraman S, Ablasser A. The cGAS-STING pathway as a therapeutic target in inflammatory diseases. *Nat Rev Immunol*. 2021;21(9):548–569. doi:10.1038/s41577-021-00524-z
7. Paul BD, Snyder SH, Bohr VA. Signaling by cGAS-STING in neurodegeneration, neuroinflammation, and aging. *Trends Neurosci*. 2021;44 (2):83–96. doi:10.1016/j.tins.2020.10.008
8. Hopfner KP, Hornung V. Molecular mechanisms and cellular functions of cGAS-STING signalling. *Nat Rev Mol Cell Biol*. 2020;21(9):501–521. doi:10.1038/s41580-020-0244-x
9. Yu CH, Davidson S, Harapas CR, et al. TDP-43 triggers mitochondrial DNA release via mPTP to activate cGAS/STING in ALS. *Cell*. 2020;183 (3):636–649. doi:10.1016/j.cell.2020.09.020
10. Zhou L, Zhang YF, Yang FH, Mao HQ, Chen Z, Zhang L. Mitochondrial DNA leakage induces odontoblast inflammation via the cGAS-STING pathway. *Cell Commun Signal*. 2021;19(1):58. doi:10.1186/s12964-021-00738-7
11. Dikalova AE, Pandey A, Xiao L, et al. Mitochondrial deacetylase Sirt3 reduces vascular dysfunction and hypertension while sirt3 depletion in essential hypertension is linked to vascular inflammation and oxidative stress. *Circ Res*. 2020;126(4):439–452. doi:10.1161/CIRCRESAHA.119.315767
12. Deng L, Liang H, Xu M, et al. STING-dependent cytosolic DNA sensing promotes radiation-induced type I interferon-dependent antitumor immunity in immunogenic tumors. *Immunity*. 2014;41(5):843–852. doi:10.1016/j.immuni.2014.10.019
13. Zhang C, Shang G, Gui X, Zhang X, Bai XC, Chen ZJ. Structural basis of STING binding with and phosphorylation by TBK1. *Nature*. 2019;567 (7748):394–398. doi:10.1038/s41586-019-1000-2
14. Jiang PY, Zhu XJ, Zhang YN, Zhou FF, Yang XF. Protective effects of apigenin on LPS-induced endometritis via activating Nrf2 signaling pathway. *Microb Pathog*. 2018;123:139–143. doi:10.1016/j.micpath.2018.06.031
15. Zhao G, Jiang K, Yang Y, et al. The potential therapeutic role of miR-223 in bovine endometritis by targeting the NLRP3 inflammasome. *Front Immunol*. 2018;9:1916. doi:10.3389/fimmu.2018.01916
16. Murakami K, Kamimura D, Hasebe R, et al. Rhodobacter azotoformans LPS (RAP99-LPS) is a TLR4 agonist that inhibits lung metastasis and enhances TLR3-mediated chemokine expression. *Front Immunol*. 2021;12:675909. doi:10.3389/fimmu.2021.675909
17. Zhang H, Wu ZM, Yang YP, et al. Catalpol ameliorates LPS-induced endometritis by inhibiting inflammation and TLR4/NF-kappaB signaling. *J Zhejiang Univ Sci B*. 2019;20(10):816–827. doi:10.1631/jzus.B1900071
18. Li R, Maimai T, Yao H, et al. Protective effects of polydatin on LPS-induced endometritis in mice. *Microb Pathog*. 2019;137:103720. doi:10.1016/j.micpath.2019.103720
19. Liu H, Song J, Zhang F, et al. A new hysteroscopic scoring system for diagnosing chronic endometritis. *J Minim Invasive Gynecol*. 2020;27 (5):1127–1132. doi:10.1016/j.jmig.2019.08.035
20. Motwani M, Pesiridis S, Fitzgerald KA. DNA sensing by the cGAS-STING pathway in health and disease. *Nat Rev Genet*. 2019;20(11):657–674. doi:10.1038/s41576-019-0151-1
21. Guo Y, Gu R, Gan D, Hu F, Li G, Xu G. Mitochondrial DNA drives noncanonical inflammation activation via cGAS-STING signaling pathway in retinal microvascular endothelial cells. *Cell Commun Signal*. 2020;18(1):172. doi:10.1186/s12964-020-00637-3
22. Li N, Zhou H, Wu H, et al. STING-IRF3 contributes to lipopolysaccharide-induced cardiac dysfunction, inflammation, apoptosis and pyroptosis by activating NLRP3. *Redox Biol*. 2019;24:101215. doi:10.1016/j.redox.2019.101215
23. Moriyama M, Koshiba T, Ichinohe T. Influenza A virus M2 protein triggers mitochondrial DNA-mediated antiviral immune responses. *Nat Commun*. 2019;10(1):4624. doi:10.1038/s41467-019-12632-5
24. Reinert LS, Rashidi AS, Tran DN, et al. Brain immune cells undergo cGAS/STING-dependent apoptosis during herpes simplex virus type 1 infection to limit type I IFN production. *J Clin Invest*. 2021;131(1). doi:10.1172/JCI136824
25. King KR, Aguirre AD, Ye YX, et al. IRF3 and type I interferons fuel a fatal response to myocardial infarction. *Nat Med*. 2017;23(12):1481–1487. doi:10.1038/nm.4428
26. Arwert EN, Milford EL, Rullan A, et al. STING and IRF3 in stromal fibroblasts enable sensing of genomic stress in cancer cells to undermine oncolytic viral therapy. *Nat Cell Biol*. 2020;22(7):758–766. doi:10.1038/s41556-020-0527-7
27. Ghosh M, Saha S, Bettke J, et al. Mutant p53 suppresses innate immune signaling to promote tumorigenesis. *Cancer Cell*. 2021;39(4):494–508. doi:10.1016/j.ccell.2021.01.003
28. Gaidt MM, Ebert TS, Chauhan D, et al. The DNA inflammasome in human myeloid cells is initiated by a STING-cell death program upstream of NLRP3. *Cell*. 2017;171(5):1110–1124. doi:10.1016/j.cell.2017.09.039
29. Spinelli JB, Haigis MC. The multifaceted contributions of mitochondria to cellular metabolism. *Nat Cell Biol*. 2018;20(7):745–754. doi:10.1038/s41556-018-0124-1
30. Wong YC, Kim S, Peng W, Krainc D. Regulation and function of mitochondria-lysosome membrane contact sites in cellular homeostasis. *Trends Cell Biol*. 2019;29(6):500–513. doi:10.1016/j.tcb.2019.02.004
31. Wang Y, Shi P, Chen Q, et al. Mitochondrial ROS promote macrophage pyroptosis by inducing GSDMD oxidation. *J Mol Cell Biol*. 2019;11 (12):1069–1082. doi:10.1093/jmcb/mjz020
32. Sun K, Jing X, Guo J, Yao X, Guo F. Mitophagy in degenerative joint diseases. *Autophagy*. 2021;17(9):2082–2092. doi:10.1080/15548627.2020.1822097
33. Maekawa H, Inoue T, Ouchi H, et al. Mitochondrial damage causes inflammation via cGAS-STING signaling in acute kidney injury. *Cell Rep*. 2019;29(5):1261–1273 e6. doi:10.1016/j.celrep.2019.09.050
34. Rao SP, Sharma N, Kalivendi SV. Embelin averts MPTP-induced dysfunction in mitochondrial bioenergetics and biogenesis via activation of SIRT1. *Biochim Biophys Acta Bioenerg*. 2020;1861(3):148157. doi:10.1016/j.bbabio.2020.148157
35. Bhargava P, Schnellmann RG. Mitochondrial energetics in the kidney. *Nat Rev Nephrol*. 2017;13(10):629–646. doi:10.1038/nrneph.2017.107
36. Margulies SL, Dhingra I, Flores V, et al. The diagnostic criteria for chronic endometritis: a survey of pathologists. *Int J Gynecol Pathol*. 2021;40 (6):556–562. doi:10.1097/PGP.0000000000000737
37. Margulies SL, Flores V, Parkash V, Pal L. Chronic endometritis: a prevalent yet poorly understood entity. *Int J Gynaecol Obstet*. 2022;158 (1):194–200. doi:10.1002/ijgo.13962